

## Synthesis, Spectroscopic Characterization, Antibacterial and Corrosion Inhibitory Activities of Some 3d-Metal Complexes of [(2-Pyrrole-2-carboxaldehyde)-3-isatin]bishydrazone

S.S. SWATHY<sup>1,\*</sup>, R. BIJU<sup>1</sup> and K. MOHANAN<sup>2</sup>

<sup>1</sup>Department of Chemistry, Sree Narayana College, Varkala, Trivandrum-695 145, India

<sup>2</sup>Department of Chemistry, University of Kerala, Kariavattom Campus, Trivandrum-695 581, India

\*Corresponding author: E-mail: [rajendran.biju@gmail.com](mailto:rajendran.biju@gmail.com)

Received: 15 May 2015;

Accepted: 27 June 2015;

Published online: 29 August 2015;

AJC-17528

A novel bishydrazone was synthesized by the condensation of isatin monohydrazone with pyrrole-2-carboxaldehyde, which formed a series of complexes with manganese(II), cobalt(II), nickel(II), copper(II) and zinc(II). The ligand and the metal complexes were characterized on the basis of elemental analysis, molar conductance, magnetic moment, IR, UV-visible, <sup>1</sup>H NMR, EPR and thermal analysis. Spectral studies revealed that the ligand acted as neutral bidentate, coordinating to the metal ion through the aldimine nitrogen and carbonyl oxygen atom of the isatin moiety. The low molar conductance values indicate that all complexes are non-electrolytes. Based on the spectral results and magnetic susceptibility measurements, suitable geometry was proposed for each metal complex. The EPR spectral data of copper(II) complex indicated that metal-ligand bond had considerable covalent character. The ligand and its nickel(II) complex were subjected to XRD studies. *In vitro* biological screening effects of the compounds were tested against the some selected bacteria by the agar disc diffusion method. The corrosion inhibitory activity of the ligand and its nickel(II) complex used in acid (H<sub>2</sub>SO<sub>4</sub>) media was examined by open circuit potential measurements.

**Keywords:** Hydrazone, Spectral studies, Cyclic voltammetry, Antibacterial activity.

### INTRODUCTION

Hydrazones form an interesting class of chelating ligands which contain an azomethine group linked to a nitrogen atom and find extensive application in various fields<sup>1-6</sup>. The interest in the study of hydrazones possessing potential donor sites have been intensively increasing because of their coordination capability, their pharmacological activity and their use in analytical chemistry as metal extracting agents<sup>7-9</sup>. The coordination behaviour of hydrazones depends on several factors such as pH of the medium, nature of the substituent and position of hydrazone group relative to other nucleus.

A thorough survey of literature on pyrrole-2-carboxaldehyde complexes reveals that metal complexes of bishydrazones derived from pyrrole-2 carboxaldehyde have been largely neglected. The compounds containing isatin moiety possess interesting biological and pharmacological activities<sup>10-13</sup>. This paper is devoted to the synthesis, characterization, X-ray diffraction and cyclic voltammetric studies on some 3d metal complexes in their +2 oxidation states with a bishydrazone formed from isatin monohydrazone and pyrrole-2-carboxaldehyde to form a potentially neutral bidentate bishydrazone viz. [(2-pyrrole-2-carboxaldehyde)-3-isatin]bishydrazone (IPB).

### EXPERIMENTAL

All chemicals used were of analytical grade. Isatin, hydrazine hydrate (99 %) and pyrrole-2-carboxaldehyde were obtained from Fluka and Sisco Chemicals.

**Synthesis of isatin monohydrazone:** A solution of hydrazine hydrate (0.5 mL, 10 mmol) dissolved in hot methanol (10 mL) was added to isatin (1.47 g, 10 mmol) dissolved in methanol (40 mL). The resulting solution was refluxed for 3 h on a water-bath and the yellow coloured compound was separated out on cooling. It was filtered, dried in vacuum and further purified by recrystallization from methanol (m.p. 226 °C; yield 95 %).

**Synthesis of bishydrazone [(2-(pyrrole-2-carboxaldehyde)-3-isatin]bishydrazone):** A solution of pyrrole-2-carboxaldehyde (0.01 mol) in methanol (10 mL) was added to a solution of isatin monohydrazone (0.01 mol) in hot methanol (50 mL). The reaction mixture was boiled under reflux for 4 h. It was reduced to half of its volume, cooled and allowed to crystallize. Orange crystals formed was filtered, washed several times with methanol and dried in vacuum over P<sub>4</sub>O<sub>10</sub> (m.p. 219 °C).

#### Synthesis of metal complexes

**Manganese(II) complex:** Manganese(II) acetate (0.001 mol) dissolved in minimum quantity of methanol was added

to a hot solution of the ligand (0.002 mol) in methanol (60 mL) with constant stirring. The pH of the solution was maintained between 6.5 and 7.5 by adding alcoholic ammonia solution. The reaction mixture was then refluxed on a water-bath for 5 h. Then it was concentrated to half of its initial volume by evaporation. On cooling the solution, the separated complex was filtered off, washed with methanol and then dried in vacuum.

**Cobalt(II) complex:** Cobalt(II) complex was prepared according to the procedure similar to that followed for the synthesis of manganese(II) complex, except the refluxing time was about for 4 h and the pH was adjusted to about 6.0. The reddish brown solid product was filtered off, washed several times with methanol and dried in vacuum.

**Nickel(II) complex:** Nickel(II) complex was prepared by employing the same procedure for the preparation of manganese(II) complex, except that the pH was maintained at about 6.5. On adding the nickel(II) chloride, the ligand solution turned to light brown colour. The metal-ligand ratio was maintained to be 1:2 and the reaction mixture was refluxed for 3-4 h. The final solution was concentrated to half of its initial volume by evaporation and then cooled. The product formed was filtered, washed successively with methanol and dried in vacuum.

**Copper(II) complex:** Copper(II) chloride (0.002 mol) dissolved in minimum quantity of methanol was added to a hot solution of the ligand (0.002 mol) in methanol (60 mL). The pH of the solution was maintained between 6.5 and 7.5, by adding alcoholic ammonia solution and heated under reflux for 2-3 h. The reaction mixture was then reduced to half of its original volume by evaporation and was allowed to cool. The complex separated out was filtered, washed with methanol, ether and finally dried in vacuum.

**Zinc(II) complex:** Zinc(II) chloride complex was prepared by the same method explained for the synthesis of copper(II) complex. The metal-ligand ratio was maintained to be 1:1 and the pH of solution was adjusted to about 7.5 by adding alcoholic ammonia solution. The reaction mixture was then refluxed for about 6 h. On cooling the final solution after evaporation to half of its original volume, the complex obtained was filtered, washed with methanol and then dried in vacuum.

**Physical measurements:** Elemental analysis (C, H and N) was carried out using a Heracus Carlo Erba 1108-CHN Analyzer. The metal contents in the complexes were analyzed using an atomic absorption spectrometer (GBC Avanta). The electronic spectra were recorded on Hitachi 320 UV-visible spectrometer in the range 200-900 nm. Infrared spectra of the ligand and the metal complexes were recorded on a Jasco

FTIR-410 spectrometer using KBr pellets and far infrared in the 500-100  $\text{cm}^{-1}$  region using CsI-discs on a polytech FIR 30 Fourier spectrometer. Proton NMR spectra of the ligand and its zinc(II) complex were recorded in DMSO- $d_6$  on a JEOL GSX 400 NB 400 MHz FT-NMR spectrometer. Molar conductance measurements were conducted using  $10^{-3}$  M solution of the complexes in DMSO at room temperature with a Systronics model 304 digital conductivity meter. Magnetic measurements of the metal complexes were performed on a Magway MSB Mk1 magnetic susceptibility balance. The EPR spectrum of the copper(II) complex was recorded using a Varian E-112 EPR spectrometer. The XRD patterns of the ligand and its nickel(II) complex were recorded on a Rigaku Dmax X-ray diffractometer using  $\text{CuK}\alpha$  radiation ( $\lambda = 1.5404 \text{ \AA}$ ).

**In vitro antibacterial activity:** The *in vitro* antibacterial activity of the ligand and its complexes were tested against the bacterial species, *Staphylococcus aureus*, *Escherichia coli* and *Salmonella typhi* by agar disc diffusion method<sup>14</sup>. Streptomycin was used as standard for antibacterial agents. The standard samples of antibacterial activity are done at 100  $\mu\text{g}/\text{mL}$  concentration in DMSO. The test organisms were grown on nutrient agar medium in petri plates. The antibacterial activities of the ligand and its metal complexes were done at 50, 100 and 200  $\mu\text{g}/\text{mL}$  concentration in DMSO solvent by the minimum inhibitory concentration (MIC) method. The discs were placed on the previously seeded plates and incubated at 37  $^{\circ}\text{C}$ . The diameter of inhibition zone around each disc was measured after 24 h for bacterial species. Activity was determined by measuring the diameter of the zone showing complete inhibition (mm).

**Open circuit potential (OCP) measurements:** The pretreated coupons were weighed and suspended vertically for 15 days in 100 mL aerated, unstirred 1 M  $\text{H}_2\text{SO}_4$  with and without the corrodent-inhibitor of different concentrations varying from  $10^{-3}$  to  $5 \times 10^{-3}$  g. The coupons were then removed and washed with 20 % NaOH solution containing 200  $\text{g L}^{-1}$  of zinc dust in order to remove the corrosion products, dried in acetone. The electrolytes were kept under stagnant condition. The potential were measured for 15 days under open circuit condition as a function of time against a saturated calomel electrode.

## RESULTS AND DISCUSSION

**Structure of ligand:** The bishydrazone was characterized through elemental analysis and various spectral studies. Analytical data and other details of the ligand are given in Table-1. The purity of the ligand was checked by TLC technique (silica gel).

TABLE-1  
ANALYTICAL DATA OF THE LIGAND (IPB) AND ITS DIVALENT METAL COMPLEXES

Compound	Yield (%)	Elemental analysis (%): Found (calcd.)				Molar conductance ( $\Omega^{-1} \text{cm}^2 \text{mol}^{-1}$ ) DMSO	$\mu_{\text{eff}}$ (BM)
		C	H	N	M		
IPB	77	65.27 (65.54)	4.12 (4.20)	23.45 (23.53)	–	–	–
[Mn(IPB) <sub>2</sub> (OAc) <sub>2</sub> ]	78	55.61 (55.48)	4.12 (4.01)	17.25 (17.26)	8.24 (8.46)	5.9	5.78
[Co(IPB) <sub>2</sub> Cl <sub>2</sub> ]	85	51.38 (51.49)	3.21 (3.30)	18.58 (18.48)	9.74 (9.72)	9.0	4.84
[Ni(IPB) <sub>2</sub> Cl <sub>2</sub> ]	88	51.64 (51.51)	3.28 (3.30)	18.53 (18.49)	9.56 (9.68)	9.2	3.12
[Cu(IPB)Cl <sub>2</sub> ]	82	41.88 (41.87)	2.64 (2.68)	15.01 (15.03)	17.16 (17.06)	7.4	1.81
[Zn(IPB)Cl <sub>2</sub> ]	80	41.59 (41.67)	2.62 (2.67)	14.88 (14.96)	17.48 (17.47)	8.3	Diamagnetic

The electronic spectrum of the bishydrazone ligand show absorption bands at 30303  $\text{cm}^{-1}$  and 35842  $\text{cm}^{-1}$  assignable to  $n \rightarrow \pi^*$  transitions of the ketimine and aldimine moieties, respectively. Infrared spectrum of the bishydrazone exhibit a absorption peak at 3358  $\text{cm}^{-1}$ , which can be attributed to N-H group of the pyrrole moiety. Another band observed at 3157  $\text{cm}^{-1}$  of medium intensity, can be assignable to (N-H) vibrations of the indole ring system. A sharp band appearing at 1686  $\text{cm}^{-1}$  is assigned to the  $>\text{C}=\text{O}$  group of the isatin moiety<sup>15</sup>. Vibrational characteristics of ketimine and aldimine groups are observed at 1588 and 1551  $\text{cm}^{-1}$  respectively. The band observed at 981  $\text{cm}^{-1}$  corresponds to the hydrazinic  $\nu(\text{N-N})$  stretching vibration.

$^1\text{H}$  NMR spectrum of the ligand (Fig. 1) gave a signal at 10.67  $\delta$  characteristic of pyrrole ring (NH). Signals appearing at 8.75  $\delta$  and 9.56  $\delta$  can be attributed to the azomethine proton and NH protons of the indole ring, respectively. Signals due to aromatic proton are observed as multiplet in the range 6.82 to 7.36  $\delta$ . On the basis of the above spectral data, the structure as in Fig. 2 has been assigned for the ligand.

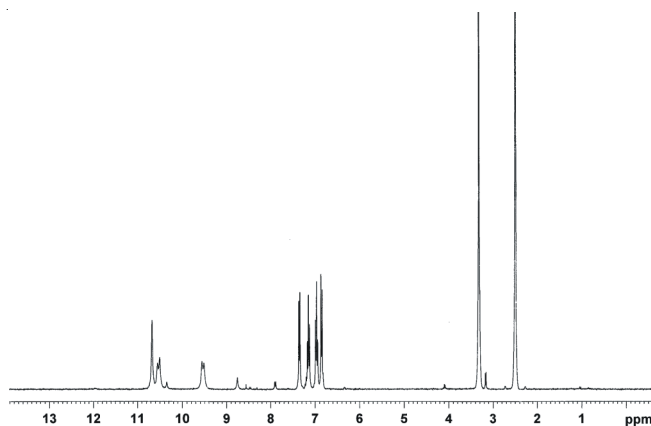


Fig. 1.  $^1\text{H}$  NMR spectrum of the ligand (IPB)

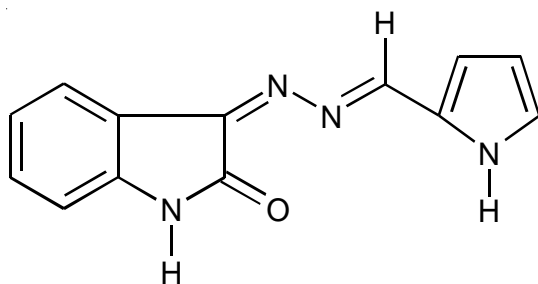


Fig. 2. Structure of the ligand

**Formation of divalent metal complexes:** Formation of metal complexes can be represented by the following general formulas (1) and (2).



All the complexes are stable in ambient condition. The analytical results obtained are in good agreement with the calculated values for the suggested formula. The ligand is soluble in common organic solvents, but the complexes are found to be insoluble except in DMSO and DMF. The low molar conductance values of the metal complexes in DMSO indicate their non-electrolytic nature.

**Infrared spectra:** Infrared spectral data of the complexes are presented in Table-2 along with their tentative assignments. The band at 3358  $\text{cm}^{-1}$  for pyrrole N-H in the free ligand remains more or less at the same position, indicating that this group did not take part in complexation. The  $\nu(\text{C}=\text{N})$  vibration of the ligand undergoes a bathochromic shift about 25  $\text{cm}^{-1}$  in the complexes due to the conjugation of the  $p$ -orbital on the double bond with the  $d$ -orbital on metal ion with reduction of the force constant, indicating involvement of the azomethine nitrogen in chelation with the metal ion. The band observed due to  $\nu(\text{C}=\text{O})$  at 1686  $\text{cm}^{-1}$  is shifted to a lower frequency by about 25-35  $\text{cm}^{-1}$ , supporting the coordination of the carbonyl oxygen. The  $\nu(\text{N-N})$  band exhibited a higher frequency shift of 12-14  $\text{cm}^{-1}$ , which is attributed to the electron attracting inductive effect, when forming the conjugated system<sup>16</sup>. However, the bands assignable to  $\nu(\text{N-H})$  of the indole ring remain more or less at the same position, indicating that this group did not take part in chelation. In the far-IR region, the appearance of new band in the regions 538-529, 490-479 and 325-319  $\text{cm}^{-1}$  can be assigned to  $\nu(\text{M-O})$ ,  $\nu(\text{M-N})$  and  $\nu(\text{M-Cl})$  vibrations respectively<sup>17-19</sup>. For the manganese(II) complex, characteristic vibrations for acetate have been observed at 1560 and 1416  $\text{cm}^{-1}$  due to  $\nu_a(\text{COO})$  and  $\nu_s(\text{COO})$ , respectively<sup>20</sup>.

These observations reveal that the ligand binds the metal ion in a bidentate manner coordinating through aldimine nitrogen and the carbonyl oxygen ( $\text{C}=\text{O}$ ) of the isatin moiety.

**$^1\text{H}$  NMR spectrum:** The proton NMR spectrum of the zinc(II) complex recorded in  $\text{DMSO-}d_6$  is shown in Fig. 3. The signal at 10.67  $\delta$  in the  $^1\text{H}$  NMR spectrum of the ligand due to NH proton of the pyrrole ring appeared at the same

TABLE-2  
KEY IR SPECTRAL BANDS ( $\text{cm}^{-1}$ ) OF THE LIGAND (IPB) AND ITS DIVALENT METAL COMPLEXES

IPB	[Mn(IPB) <sub>2</sub> (OAc) <sub>2</sub> ]	[Co(IPB) <sub>2</sub> Cl <sub>2</sub> ]	[Ni(IPB) <sub>2</sub> Cl <sub>2</sub> ]	[Cu(IPB)Cl <sub>2</sub> ]	[Zn(IPB)Cl <sub>2</sub> ]	Tentative assignments
3358	3359	3360	3357	3359	3356	Pyrrole ring N-H
3157	3158	3155	3156	3157	3154	Indole ring N-H
1686	1652	1656	1653	1657	1661	$\nu(\text{C}=\text{O})$ ring
1588	1588	1586	1582	1584	1587	$\nu(\text{C}=\text{N})$ ring
1552	1526	1527	1524	1525	1523	$\nu(\text{C}=\text{N})$ aldimine
981	995	994	995	993	993	$\nu(\text{N-N})$
—	479	481	490	485	489	$\nu(\text{M-N})$
—	536	538	537	529	534	$\nu(\text{M-O})$
—	323	325	319	320	322	$\nu(\text{M-Cl})$

position in the spectrum of the complex. This is a clear indication that the NH proton of the pyrrole ring did not take part in complexation<sup>21</sup>. Also in the ligand spectrum, a peak at 8.75  $\delta$  has been assigned for the hydrogen of the azomethine moiety and is shifted to 8.59  $\delta$  in the complex indicating the involvement of azomethine group [CH=N-] in complex formation. The protons due to benzene and indole rings are found to be in the expected region and shifted slightly by about 0.10-0.20  $\delta$  due to the coordination of the ligand to the metal ion.

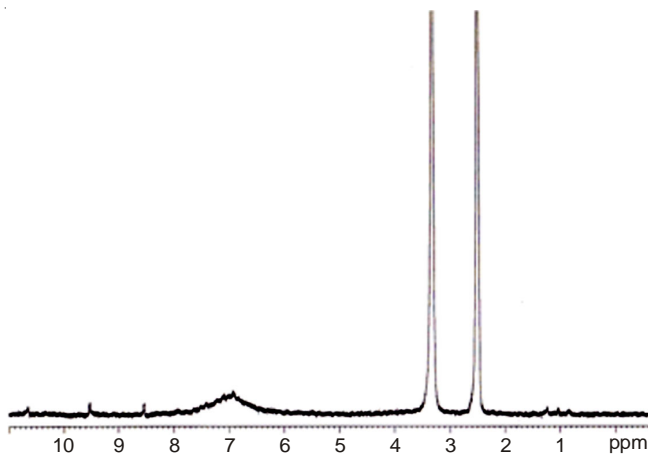


Fig. 3. <sup>1</sup>H NMR spectrum of zinc(II) complex

#### Electronic spectra and magnetic susceptibility measurements:

The electronic spectra of manganese(II) complex shows absorption bands at 14,100, 16,500 and 19,650  $\text{cm}^{-1}$ , which are due to charge transfer and  ${}^6A_{1g} \rightarrow {}^4T_{1g}$ ,  ${}^6A_{1g} \rightarrow {}^4T_{2g}$  and  ${}^6A_{1g} \rightarrow {}^4E_g$ ,  ${}^4A_{1g}$  transitions, respectively<sup>22</sup>. These data along with magnetic moment value of manganese(II) complex indicates an octahedral environment around the metal ion.

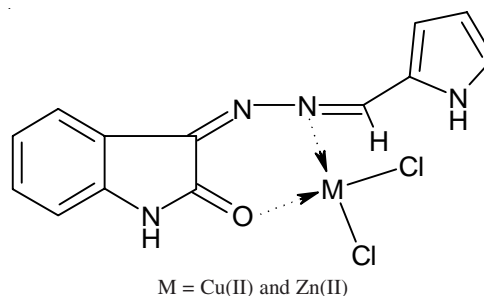
Cobalt(II) complex exhibits bands at 7,300, 17,241 and 20,449  $\text{cm}^{-1}$  assignable to  ${}^4T_{1g}(F) \rightarrow {}^4T_{2g}(F)$ ,  ${}^4T_{1g}(F) \rightarrow {}^4A_{2g}(F)$  and  ${}^4T_{1g}(F) \rightarrow {}^4T_{2g}(P)$  transitions, respectively<sup>23,24</sup>. Tetrahedral cobalt(II) complexes have generally lower magnetic moment values of the range 4.20-4.58 BM. But the magnetic moment values for the corresponding octahedral complexes are around 4.8 BM and also the observed electronic spectral data for the present cobalt(II) complex is comparable with an octahedral geometry around the metal ion.

The electronic spectra of nickel(II) complex show three peaks at 25,500, 17,200 and 9,750  $\text{cm}^{-1}$  which are assigned to  ${}^3A_{2g}(F) \rightarrow {}^3T_{1g}(P)$ ,  ${}^3A_{2g}(F) \rightarrow {}^3T_{1g}(F)$  and  ${}^3A_{2g}(F) \rightarrow {}^3T_{2g}(P)$  transitions, respectively. These transitions along with magnetic moment value suggest an octahedral geometry for the nickel(II) complex<sup>25</sup>. The copper(II) complex exhibits a broad band centered at 13,500  $\text{cm}^{-1}$  due to  ${}^2B_{1g} \rightarrow {}^2A_{1g}$  transitions of a distorted square planar geometry. These observations together with the magnetic moment value of 1.81 BM, support a distorted square planar geometry for the copper(II) complex.

Analytical data, molar conductance values and diamagnetic nature, adequately support a tetrahedral geometry for the zinc(II) complex. The completely filled *d*-orbitals in zinc(II) and the absence of LFSE seem largely responsible for the much less extensive coordination chemistry of zinc(II). The zinc(II) ion is flexible with respect to the number of ligands it can

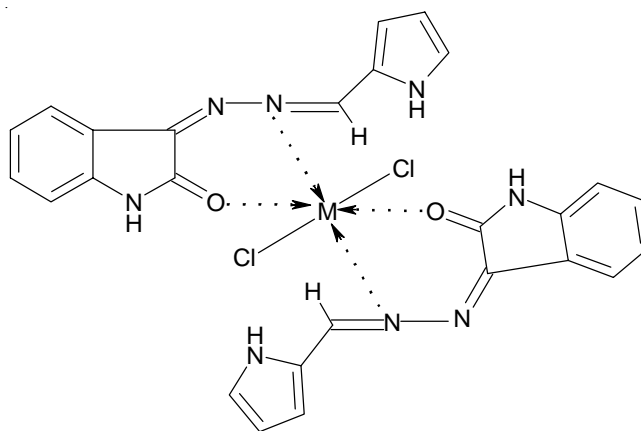
adopt in its coordination shell. It is reported that tetrahedral geometry is the most preferred structure for four coordinated zinc(II) complex<sup>26</sup>.

From the above spectral data, the structures as in Figs. 4 and 5 have been assigned for the metal complexes.



M = Cu(II) and Zn(II)

Fig. 4. Structure of 1:1 metal complexes



M = Ni(II), Co(II), Mn(II)

Fig. 5. Structure of 1:2 metal complexes

**EPR spectrum:** The X-band EPR spectra of the copper(II) complex provides information of the metal ion environment. It has been recorded in solid state room temperature. The spectrum at room temperature itself shows axial spectrum. The  $g_{\parallel}$  and  $g_{\perp}$  values have been found to be 2.2350 and 2.0601, respectively. The  $g_{av}$  value is 2.1184. The trend  $g_{\parallel} > g_{\perp} > 2.0027$  observed for the complexes indicate that the unpaired electron is localized in the  $d_{x^2-y^2}$  orbital of the copper(II) ion and are characteristic for the axial symmetry. The fact that the unpaired electron lies predominately in the  $d_{x^2-y^2}$  orbital is also supported by the value of exchange interaction term *G* estimated from the expression<sup>27</sup>.

$$G = (g_{\parallel} - 2.0027)/(g_{\perp} - 2.0027)$$

If  $G > 4.0$ , the local axes are aligned parallel or only slightly misaligned. If  $G < 4.0$ , significant exchange coupling is present and the misalignment is appreciable. The observed value for the exchange interaction parameter for the copper(II) complex ( $G = 4.0470$ ) suggests that the local tetragonal axes are aligned parallel or slightly misaligned and that the unpaired electron is present in the  $d_{x^2-y^2}$  orbital.

**XRD studies:** The X-ray diffraction pattern of the ligand (Fig. 6) indicates its high crystallinity. The diffractogram shows 10 reflections for  $2\theta$  value ranging from 12° to 33° with maxima at  $2\theta = 13.29403$  which corresponds to interplanar

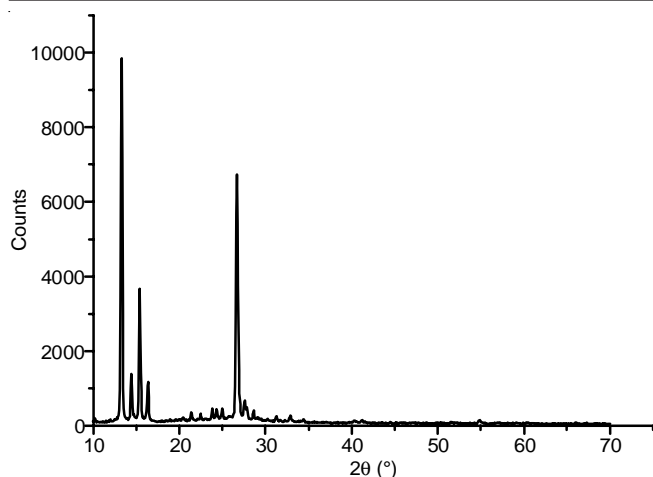


Fig. 6. XRD pattern of the ligand (IPB)

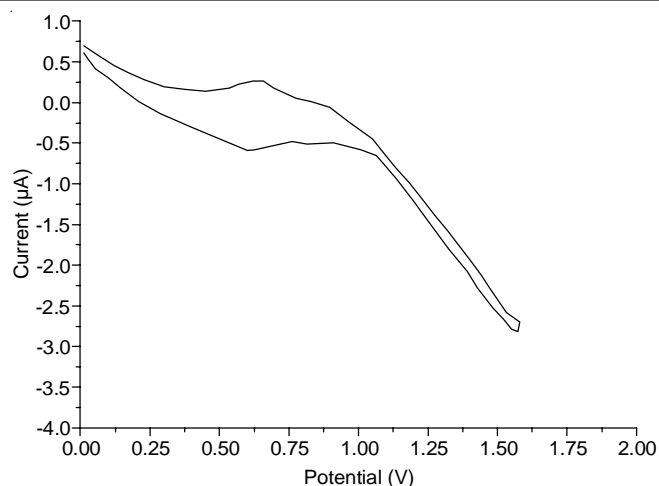


Fig. 7. Cyclic voltammogram of copper(II) complex

distance  $d = 6.6546 \text{ \AA}$ . The main peaks have been indexed using the XRDA software and the data obtained are tabulated in Table-3. The observed  $\sin^2 \theta$  and  $2\theta$  values obtained have been compared with the calculated values<sup>28</sup>.

A comparison of these values shows good agreement between observed and calculated values. Hence the ligand is successfully indexed to orthorhombic crystal system with the lattice constant unit cell parameters are;  $a = 16.16492 \text{ \AA}$ ,  $b = 11.73966 \text{ \AA}$  and  $c = 8.68687 \text{ \AA}$ . The unit cell volume is found to be  $1,648.5 \text{ \AA}^3$ . On complexation, crystallinity of the ligand has been lost and the complex becomes amorphous in nature.

**Cyclic voltammetric studies:** The copper(II) complex of IPB has been subjected to cyclic voltammetric study. The CV profile (Fig. 7) of  $[\text{Cu}(\text{IPB})\text{Cl}_2]$  complex, has displayed a wave at  $E_{\text{pa}}$  value  $+0.60 \text{ V}$ , due to the oxidation of Cu(I) to Cu(II) and  $E_{\text{pc}}$  value at  $+0.67 \text{ V}$ , which is attributed to the reduction of Cu(II). The peak separation ( $\Delta E_p$ ) is found to be  $75 \text{ mV}$  ( $\Delta E_p$  greater than  $59$  indicates irreversible reaction) indicating one electron transfer in the electrode reaction. The ratio of the anodic to cathodic peak current ( $I_{\text{pa}}/I_{\text{pc}}$ ) approaches to one<sup>29,30</sup>. Thus from the above voltammetric data electrochemical process is  $[\text{Cu}^{\text{II}}(\text{IPB})\text{Cl}_2] + 1e^- \rightarrow [\text{Cu}^{\text{I}}(\text{IPB})\text{Cl}] + \text{Cl}^-$ . Here, the electrochemical process is diffusion controlled. The decomplexation and copper metal deposition on the electrode have not been observed<sup>31</sup>.

**Corrosion inhibition activity:** Corrosion inhibition is attributed to the adsorption of inhibitors on mild steel. The open circuit decay of mild steel coupon immersed in  $1 \text{ M H}_2\text{SO}_4$  for 15 days with and without the corrodent-inhibitor of

varying concentration from  $1 \times 10^{-3}$  to  $5 \times 10^{-3} \text{ g}$  is measured and compared. Apart from this, the ligand is found to possess more inhibitory action than the metal complex. The inhibition efficiency increases with increase in concentration of the additives. The lone pair of electrons of nitrogen and oxygen atoms along with the delocalized  $p$ -electron can be the reason for higher inhibition efficiency<sup>32</sup>. These factors play the vital role in the adsorption of the inhibitor and the formation of coordinate bond with metal. The adsorption of inhibitor on the mild steel surface can occur either directly by the interactions between the  $\pi$ -electrons of the inhibitor and the vacant  $d$ -orbitals of metal surface atoms. The adsorption of inhibitor on mild steel may also be due to the interaction of nitrogen and oxygen with the surface atoms of metal. As inhibitor concentration increases, it covers more and more surface area and results in the reduction of corrosion rate<sup>33</sup>. Fig. 8 shows the trend of open circuit potential decay with and without the corrodent inhibitor (Table-4) of varying concentration from  $10^{-3}$  to  $5 \times 10^{-3} \text{ g}$  for 15 days. The open circuit potential decay of a mild steel coupon kept in a blank cell *i.e.* without inhibitor ( $1 \text{ M H}_2\text{SO}_4$ ) is also given in Fig. 8 to understand the extent of open circuit potential deviation due to the presence of the inhibitor. In the case of blank solution the initial open circuit potential value instantly changes to a negative value as high as  $-0.925 \text{ mV}$  which shows severe corrosion attack. However the addition of different concentration of the ligand and complex to the solution is able to bring the potential values towards positive region. This is due to the ability of the ligand complex solution to form a passive film on the surface of mild

TABLE-3  
X-RAY DIFFRACTION DATA OF LIGAND

Peak No.	$d$ (Å)	Observed ( $2\theta$ )	Calculated ( $2\theta$ )	Observed ( $\sin^2 \theta$ )	Calculated ( $\sin^2 \theta$ )	hkl
1	6.65460	13.29403	13.28376	0.013385	0.013378	210
2	6.13132	14.43433	14.53374	0.015767	0.016000	120
3	5.41665	16.35104	16.43162	0.020202	0.020421	003
4	4.34307	20.43184	20.42266	0.031424	0.031428	002
5	4.14836	21.40192	21.29546	0.034440	0.034140	221
6	3.73717	23.78932	23.79427	0.042440	0.042500	220
7	3.64953	24.36926	24.44097	0.044503	0.044806	122
8	3.55991	24.99258	24.94269	0.046772	0.046635	202
9	3.23354	27.56247	27.80000	0.056690	0.057711	222
10	2.85964	31.25268	31.34682	0.072484	0.072983	103

TABLE-4  
VARIATION OF OPEN CIRCUIT POTENTIAL DECAY FOR MILD STEEL IMMERSSED IN  
BLANK AND INHIBITOR SOLUTIONS OF IPB AND [Ni(IPB)<sub>2</sub>Cl<sub>2</sub>] COMPLEX

No. of days	Potential blank (mV)	Potential (mV) of ligand in various concentration			Potential (mV) of complex in various concentration		
		1 × 10 <sup>-3</sup> (g)	3 × 10 <sup>-3</sup> (g)	5 × 10 <sup>-3</sup> (g)	1 × 10 <sup>-3</sup> (g)	3 × 10 <sup>-3</sup> (g)	5 × 10 <sup>-3</sup> (g)
3	-0.496	-0.592	-0.582	-0.608	-0.720	-0.712	-0.707
6	-0.545	-0.583	-0.575	-0.570	-0.709	-0.705	-0.692
9	-0.623	-0.572	-0.565	-0.561	-0.682	-0.681	-0.670
12	-0.715	-0.568	-0.555	-0.552	-0.670	-0.665	-0.658
15	-0.880	-0.553	-0.548	-0.545	-0.652	-0.645	-0.639
18	-0.925	-0.544	-0.540	-0.536	-0.621	-0.612	-0.611

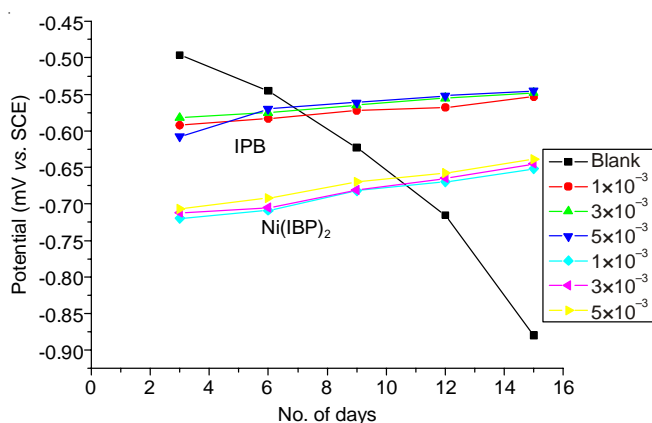


Fig. 8. Trend of open circuit potential decay for mild steel immersed in blank and inhibitor solutions of IPB and [Ni(IPB)<sub>2</sub>Cl<sub>2</sub>] complex

steel coupons. Extend of film formation is more prominent in the ligand when compared to the complexes because the ligand is more chemical adsorptive than complexes. It can be explained on the basis of the effect of chemical structure. In this respect, the isatin ring, benzene ring, N-H, C=N and C=O of bishydrazone can form a big  $\pi$  bond accordingly, not only the  $\pi$  of benzene, C=O enter the unoccupied orbital of iron, but also the  $\pi^*$  orbital can accept the electron of  $d$  orbital of iron to form back bonds. These back bonds produce more than one centre of chemical adsorption on the mild steel surfaces<sup>34</sup>. In case of the metal complexes the chemical adsorption is less because the ligand shares its lone pair to the metal ion that will reduce the effective adsorption of mild steel surface.

**Antibacterial activity:** The *in vitro* antibacterial activity value of the compounds against the growth of micro-organisms is summarized in Table-5. Inhibition is found to increase with increase in concentration of metal complex. The results show that the metal complexes exhibit higher activity against each class of organism. The activity is related to the nature and structure of the complexes. The relation between chelation and toxicity is very complex, expected to be a function of steric, electronic and pharmacokinetic factors along with mechanistic pathways. The MIC values of some compounds, show significant activity against selected bacterial species. The results indicate that, these compounds are active in inhibiting the growth of the bacterial species. A comparative study of the ligand and its complexes indicate that the metal complex exhibit higher antibacterial activity than the free ligand. Such increased activity of the complexes can be explained on the basis of the Overtone concept and the Tweedy's chelation theory<sup>24,35</sup>. According to the Overtone concept of cell permeability,

TABLE-5  
ANTIBACTERIAL RESULTS OF THE  
INVESTIGATED COMPOUNDS OF IPB

Compound	Conc. (µg/mL)	Diameter of zones showing complete inhibition of growth (mm)		
		<i>E. coli</i>	<i>S. typhi</i>	<i>S. aureus</i>
IPB	50	4.8	4.0	3.2
	100	5.9	5.1	5.6
	200	7.6	6.8	7.1
[Mn(IPB) <sub>2</sub> (OAc) <sub>2</sub> ]	50	8.2	6.0	7.8
	100	10.6	9.0	10.9
	200	14.8	13.6	14.2
[Co(IPB) <sub>2</sub> Cl <sub>2</sub> ]	50	6.2	8.3	5.6
	100	11.2	14.3	10.5
	200	16.0	14.0	12.4
[Ni(IPB) <sub>2</sub> Cl <sub>2</sub> ]	50	–	–	8.1
	100	–	–	12.5
	200	8.6	6.2	14.1
[Cu(IPB)Cl]	50	–	4.2	7.0
	100	–	10.2	12.0
	200	12.0	15.0	13.2
[Zn(IPB)Cl]	50	8.7	9.2	7.0
	100	12.5	12.5	12.2
	200	14.6	14.0	15.2
Streptomycin <sup>a</sup>	100	30.0	31.0	32.0

<sup>a</sup>Standards

Antibacterial activity: >15 mm, significant; 10-14 mm, moderate activity; <10, weak activity.

the lipid membrane surrounding the cell favours the passage of only lipid-soluble materials, due to which liposolubility is an important factor controlling the antibacterial activity. On chelation, the polarity of the metal ion will be reduced to a greater extent due to the overlap of the ligand orbital and partial sharing of the positive charge of the metal ion with donor groups. Furthermore, the mode of action of the compound may involve formation of a hydrogen bond through the azomethine group with the active centre of cell constituents, resulting in interference with normal cell processes.

## Conclusion

A novel bishydrazone *viz.* [(2-pyrrole-2-carboxaldehyde)-3-isatin]bishydrazone and its metal complexes were synthesized and characterized on the basis of various physico-chemical and spectral studies. The ligand behaved as neutral bidentate coordinating to the metal ion through the aldimine nitrogen and carbonyl oxygen atom of the isatin moiety. On the basis of all the spectral data, it is observed that manganese(II), cobalt(II) and nickel(II) complexes possess an octahedral geometry, copper(II) complex possess a distorted square planar geometry whereas zinc(II) complex possess a tetrahedral

geometry. The XRD studies show that ligand possess crystalline nature with orthorhombic crystal lattice and but its nickel(II) complex is amorphous in nature. In view of antibacterial activity observations of hydrazone derivatives, metal complexes are found to be more potent bactericides than the ligand. Corrosion inhibition efficiency of the ligand and its nickel(II) complex reveal that the ligand possess greater activity than the metal complex.

#### ACKNOWLEDGEMENTS

The authors express their sincere thanks to Prof. and Head, Department of Chemistry, University of Kerala, Kariavattom Campus, Trivandrum, India for providing the necessary facilities for carrying out this work. Instrumental facilities provided by SAIF, Cochin, IIT, Bombay, CDRI, Lucknow and NIIST, Trivandrum are also gratefully acknowledged.

#### REFERENCES

- M.C. Rodriguez-Argüelles, M.B. Ferrari, F. Bisceglie, C. Pelizzi, G. Pelosi, S. Pinelli and M. Sassi, *J. Inorg. Biochem.*, **98**, 313 (2004).
- S.K. Sridhar and A. Ramesh, *Biol. Pharm. Bull.*, **24**, 1149 (2001).
- P. Paciorek, J. Szklarzewicz, A. Jasińska, B. Trzewik, W. Nitek and M. Hodorowicz, *Polyhedron*, **87**, 226 (2015).
- B. Holló, J. Magyari, V. Zivkovic-Radovanovic, G. Vuckovic, Z.D. Tomic, I.M. Szilágyi, G. Pokol and K.M. Szécsényi, *Polyhedron*, **80**, 142 (2014).
- A. Taha, A.A.A. Emara, M.M. Mashaly and O.M.I. Adly, *Spectrochim. Acta A*, **130**, 429 (2014).
- A.D.M. Mohamad, M.K. Rabia, N.M. Ismail and A.A. Mahmoud, *Int. J. Chem. Kinet.*, **46**, 451 (2014).
- J.F. Alcock, R.J. Baker and A.A. Diamantis, *Aust. J. Chem.*, **25**, 289 (1972).
- J.R. Dilworth, *Coord. Chem. Rev.*, **21**, 29 (1976).
- M. Katyal and Y. Dutt, *Talanta*, **22**, 151 (1975).
- A. Ercag, S.O. Yildirim, M. Akkurt, M.U. Ozgar and F.W. Heinemann, *Chin. Chem. Lett.*, **17**, 243 (2006).
- S.N. Pandeya, D. Sriram, G. Nath and E. De Clercq, *Pharm. Acta Helv.*, **74**, 11 (1999).
- S.K. Sridhar, S.N. Pandeya, J.P. Stables and A. Ramesh, *Eur. J. Pharm.*, **16**, 129 (2002).
- L.P. Nitha, R. Aswathy, N.E. Mathews, B.S. Kumari and K. Mohanan, *Spectrochim. Acta A*, **118**, 154 (2014).
- A.W. Bauer, W.M.M. Kirby, J.C. Sherris and M. Turck, *Am. J. Clin. Pathol.*, **45**, 493 (1966).
- N. Singh, S. Hingorani, J. Srivastava, V. Puri and B.V. Agarwala, *Synth. React. Inorg. Met. Org. Chem.*, **22**, 1283 (1992).
- P.K. Singh and D.N. Kumar, *Spectrochim. Acta A*, **64**, 853 (2006).
- J.R. Ferraro, *Low Frequency Vibrations of Inorganic and Coordination Compounds*, Plenum Press, New York (1971).
- A. Çukurovali, I. Yilmaz, H. Özmen and M. Ahmedzade, *Transition Met. Chem.*, **27**, 171 (2002).
- K.C. Raju and P.K. Radhakrishnan, *Synth. React. Inorg. Met. Org. Chem.*, **33**, 1307 (2003).
- K. Nakamoto, *Infrared and Raman Spectra of Inorganic and Coordination Chemistry*, Wiley Interscience, New York (1978).
- E.M. Niecy, L.P. Nitha, R. Aswathy, B. Sindhukumari and K. Mohanan, *Med. Chem. Res.*, **24**, 63 (2015).
- R.K. Parihari, R.K. Patel and R.N. Patel, *J. Indian Chem. Soc.*, **77**, 339 (2000).
- D.N. Sathyanarayana, *Electronic Absorption Spectroscopy and Related Techniques*, University Press (India) Limited, Hyderabad, India (2001).
- K.N. Thimmaiah, W.D. Lloyd and G.T. Chandrappa, *Inorg. Chim. Acta*, **106**, 81 (1985).
- Z.H. Chohan and S. Kausar, *Chem. Pharm. Bull. (Tokyo)*, **40**, 2555 (1992).
- T. Dudev and C. Lim, *J. Am. Chem. Soc.*, **122**, 11146 (2000).
- J.T. Makode and A.S. Aswar, *J. Indian Chem. Soc.*, **80**, 44 (2003).
- S.A. Patil, S.N. Unki, A.D. Kulkarni, V.H. Naik and P.S. Badami, *J. Mol. Struct.*, **985**, 330 (2011).
- A.J. Bard and L.R. Faulkner, *Electrochemical Methods: Fundamentals and Applications*, John Wiley & Sons, New York (2000).
- R.S. Nicholson and I. Shain, *Anal. Chem.*, **36**, 706 (1964).
- G.K. Rauth and C. Sinha, *Transition Met. Chem.*, **27**, 756 (2002).
- S. Sanyal and A. Kumar, *J. Indian Chem. Soc.*, **87**, 189 (2010).
- R.S.A.E. Hameed, H.I.A. Shafey, A.S.A. Magd and H.A. Shehata, *J. Mater. Environ. Sci.*, **3**, 294 (2012).
- R.S.A.E. Hameed, *Adv. Appl. Sci. Res.*, **2**, 483 (2011).
- D. Kulkarni, S.A. Patil and P.S. Badami, *Int. J. Electrochem. Sci.*, **4**, 717 (2009).